

Robust optimal synthetic aperture imaging of towed streamer electromagnetic data

Xiaolei TU^{1*} and Michael S. Zhdanov^{1,2}; ¹University of Utah; ²TechnoImaging

Summary

The synthetic aperture (SA) method has recently found applications in analysis of the low frequency marine controlled source electromagnetic data. It has been shown in numbers of publications that SA method can enhance the response from an anomalous target. However, the SA method may not only ‘steer’ the EM field in the area of interest, but also steer the noise, thus unreasonably amplifying the noise level. In addition, the current realizations of the SA method are themselves very sensitive to the noise in the data and to the parameters of the synthetic aperture. To overcome these difficulties, we have developed a robust SA method. The synthetic model study presented here shows that this method is stable with respect to noise and has a relatively high spatial resolution.

Introduction

The SA method is one of the key techniques in remote sensing using radio frequency signals. Over the last several years this method has also been extended to the case of a low-frequency EM field used in marine geophysical exploration (e.g., Fan et al., 2010, 2012; Knaak et al., 2013; Mattsson and Engelmarm, 2013). To determine the optimal parameters of the SA method for marine EM surveys, an optimal SA (OSA) method had been developed (Yoon and Zhdanov, 2015; Zhdanov et al., 2017). One of the practical difficulties of the OSA method is that it is sensitive to the background geoelectrical model and to the noise in the data. In the present paper, we propose a robust OSA (RSA) method, which is less affected by the choice of the background model and the noise. The developed RSA method was carefully tested using synthetic model study.

SA method for the towed streamer EM survey

A towed streamer EM survey consists of a set of transmitter and receivers towed by a vessel (Zhdanov, 2018). The receiver positions for one transmitter shot are different from those for another, while the relative displacements of receivers with respect to the transmitter are the same. Consider a typical towed streamer EM survey consisting of a set of towed receivers with the transmitter-receiver offset index, $s = 1, 2, \dots, S$. A bipole transmitter generates a low-frequency EM field from the points with coordinates $r_j, j = 1, 2, \dots, J$. The data generated by a transmitter located at point r_j and recorded at the corresponding receivers can be presented as a vector-column, $\mathbf{d}_j = [d_j^{(1)}, d_j^{(2)}, \dots, d_j^{(S)}]^T$,

where $d_j^{(s)}$ is the datum observed at offset S generated by the transmitter located at the point r_j .

The SA method is based on constructing a synthetic aperture source as a superposition of the spatially distributed sources located at the points r_j (Fan et al., 2010, 2012; Yoon and Zhdanov, 2015). It has been demonstrated by Yoon and Zhdanov (2015) and Zhdanov et al. (2017) that the SA data can be calculated as a linear combination of the responses for all the transmitters:

$$\mathbf{d}_A = \mathbf{E} \mathbf{w}, \quad (1)$$

where $\mathbf{d}_A = [d_A^{(1)}, d_A^{(2)}, \dots, d_A^{(L)}]^T$ is a column of SA data; \mathbf{E} is an $[L \times J]$ matrix of the in-line components of the electric fields observed in the receivers; and \mathbf{w} is a column vector of the corresponding SA weights, $\mathbf{w} = [w_1, w_2, \dots, w_J]^T$ (index j indicates that the SA weights are transmitter dependent). Thus, we can see that, for every transmitter we assign a corresponding weight, w_j , which is in a general case a complex number. The data collected by all the receivers for one transmitter shot share the same weight. The data corresponding to different transmitter shots are then combined to form the SA data. The goal is to find the optimal values of the weights, which would enhance the EM anomalies from the target.

RSA method

This new method consists of three steps:

A. Robust Background field smoothing

In the marine environment, the measured electric field decays rapidly with increase of the distance (offset) between the transmitter and the receiver, which makes it difficult to detect an anomaly related to a hydrocarbon (HC) reservoir. In order to overcome this problem, the observed data are usually normalized by the amplitude of the background field as follows:

$$d_j^{N(s)} = d_j^{(s)} / d_j^{b(s)}, \quad (2)$$

where $d_j^{(s)}$ and $d_j^{b(s)}$ describe the total and background field data, respectively, recorded at offset s from the transmitter located at point r_j .

There are different ways to determine the background field (Zhdanov et al., 2017). One is to use a reference field in the observation point far enough from the region of interest. However, the reference field is always contaminated by acquisition noise and a response from the local anomalies,

Robust optimal synthetic aperture imaging of towed streamer electromagnetic data

which may introduce noise into the normalized fields. Denoising of the reference field is needed before application of the successive steps.

Here, we apply the robust smoothing to the background field before performing the normalization. The robust smoothing can be formalized as the minimization of the following parametric functional:

$$p^\alpha(\mathbf{d}^b, \widehat{\mathbf{d}}^b) = \|\widehat{\mathbf{d}}^b - \mathbf{d}^b\|^2 + \alpha \|\mathbf{R}\widehat{\mathbf{d}}^b\|^2 \rightarrow \min, \quad (3)$$

where $\widehat{\mathbf{d}}^b$ is the smoothed background field; \mathbf{R} is the roughness operator, which is the second order differential operator. The regularization parameter, α , tunes up the misfit-stabilizer balance. This optimization problem is solved with the reweighted regularized conjugate gradient (RRCG) method (Zhdanov, 2015). The robust smoothing is similar to a spatial low pass filter, which forces the fields to follow a general spatial trend and remove the local outliers. The environmental noise and response from the local anomalies are removed as well.

B. Robust interpolation of EM fields to Virtual receivers

One of the fundamental concept of the SA method for towed streamer EM system is that the signals measured at the different sets of real receiver positions from each source are interpolated and/or extrapolated to a set of virtual receiver positions, so that they can be integrated to increase the potential anomaly (Zhdanov et al., 2017). The set of virtual receiver positions is shared by all the transmitter shots. Note that, the concept of virtual receiver is also quite common in radar applications (Zhdanov et al., 2017).

A global interpolation operator, which we call robust smoothing interpolation, can be introduced to make the field interpolation from the actual receiver positions to the virtual receivers more robust. The robust smoothing interpolation is defined as the minimization of the following parametric functional:

$$p^\alpha(\mathbf{d}, \mathbf{d}^v) = \|\mathbf{d}^v - \mathbf{P}\mathbf{d}\|^2 + \alpha \|\mathbf{R}\mathbf{d}^v\|^2 \rightarrow \min, \quad (4)$$

where \mathbf{d}^v is the vector of the interpolated fields in the virtual receivers; \mathbf{d} is the vector of original fields in the actual receivers defined by formula (2). \mathbf{P} denotes conventional interpolation (linear or spline) operator. \mathbf{R} is the roughness operator. The optimization problem is also solved with the RRCG method. The robust smoothing interpolation is a global operator which relates the current interpolated value to not only its neighbors but also to all the sampling points involved. Thus, the interpolated field is forced to follow a general trend in the data without being affected by the local outliers. The smoothing regularization term can also help denoise the interpolated field. In this way, the fields calculated in the virtual receivers are less biased by the noise.

C. RSA weights

Following Yoon and Zhdanov (2015), the normalized SA data \mathbf{d}_R is formulized as of the ratio between the SA in-line electric fields and the background fields:

$$\mathbf{d}_R = [d_A^{(1)}/d_B^{(1)}, d_A^{(2)}/d_B^{(2)}, \dots, d_A^{(L)}/d_B^{(L)}]^T = \mathbf{A}(\mathbf{w}), \quad (5)$$

where $d_B^{(l)}$ is the element of the SA response for the background field $\mathbf{d}_B = \mathbf{E}^b\mathbf{w}$; \mathbf{A} is a forward operator for the normalized SA data, which is a function of the SA weights, \mathbf{w} . Note that, if all the SA weights, are equal to 1, then according to Zhdanov et al. (2017), the corresponding data \mathbf{d}_R are called the SA data without steering. The values \mathbf{d}_R computed based on the RSA weights are called RSA data.

The RSA weights can be found by solving a minimization problem for the corresponding parametric functional:

$$p^\alpha(\mathbf{D}, \mathbf{w}) = \|\mathbf{D} - \mathbf{A}(\mathbf{w})\|^2 + \alpha \|\mathbf{w} - \mathbf{w}_{\text{apr}}\|^2 \rightarrow \min, \quad (6)$$

where \mathbf{D} is the so-called designed SA (DSA), α is a regularization parameter, and \mathbf{w}_{apr} is an a priori vector-column of the data weights. The DSA, according to its name, is selected (designed) with the purpose of enhancing the EM anomalies from the potential targets. In the case of a reconnaissance survey, it is reasonable to select a uniform DSA with the constant value greater than one to enhance the anomalies, present in the survey area.

Note that, a priori data weights are usually not available before the SA. We instead replace the stabilizer with a smoothing regularization term:

$$p^\alpha(\mathbf{D}, \mathbf{w}) = \|\mathbf{D} - \mathbf{A}(\mathbf{w})\|^2 + \alpha \|\mathbf{R}\mathbf{A}(\mathbf{w})\|^2 \rightarrow \min, \quad (7)$$

where \mathbf{R} is the roughness operator. By introducing it, smoothed SA data are preferred. The minimization problem can be solved with the RRCG method (Zhdanov, 2015).

Once the optimal SA weights are found, the SA data \mathbf{d}_R can be easily calculated using equation (5).

Representation of the robust norms in a form of quadratic functionals

The least squares norm (L_2 norm) is the most popular error metric in geophysical inverse problem. However, it has long been understood that the basic underlying hypothesis (Gaussian uncertainties) for least squares criterion is generally not satisfied as a result of long-tailed density functions in data and model uncertainties (Tarantola, 2005).

These drawbacks of L_2 norm led to a group of robust norms, such as Huber norm, Hampel norm, and Tukey bisquare norm. Their general idea is to combine different treatments of residuals together. Usually small residuals are considered

Robust optimal synthetic aperture imaging of towed streamer electromagnetic data

more ‘important’ than big ones. The robust norm is considerably less sensitive to large measurement errors and more appropriate for a long-tailed probability density functions. The robust norm can be introduced as a weighted least-squares norm.

In a general case, arbitrary robust norm of the residual vector $\mathbf{r} = (r_1, r_2, \dots, r_n)^T$ can be given by the following formula:

$$\|\mathbf{r}\|_{\rho}^2 = \sum_{i=1}^n |\rho_i(\mathbf{r})|^2, \quad (8)$$

where $\rho_i(\mathbf{r})$ are the functions of \mathbf{r} determining the properties of the corresponding robust norm. Expression (11) can also be written as a quasi-quadratic functional as follows:

$$\|\mathbf{r}\|_{\rho}^2 = (\mathbf{W}_{\rho}\mathbf{r}, \mathbf{W}_{\rho}\mathbf{r}), \quad (9)$$

where \mathbf{W}_{ρ} is a diagonal weighting matrix of the robust norm with the components:

$$W_{\rho i}(\mathbf{r}) = \frac{\rho_i(\mathbf{r})}{(|r_i|^2 + e)^{\frac{1}{2}}}, \quad (10)$$

where $e > 0$ is a small number introduced to avoid a singularity.

For Huber norm, the $\rho_i(\mathbf{r})$ are defined as:

$$\rho_i^{Huber}(\mathbf{r}) = \begin{cases} r_i, & \text{if } |r_i| < a \\ \left(a|r_i| - \frac{1}{2}a^2\right)^{\frac{1}{2}}, & \text{if } |r_i| \geq a \end{cases}$$

Note that, the misfit functionals in equations (3), (4), and (7) are calculated with L_2 norm. We can make them more robust by employing the robust norms introduced above.

Synthetic model study

A. Robustness to noise

In this section, we discuss how the proposed method has strong resistance to the noise in the data.

Consider a geoelectrical Model 1 consisting of 300 m seawater layer with a resistivity of 0.33 Ohm-m, a 1 Ohm-m middle layer of 200 m thickness and a half space basement of 3 Ohm-m (Figure 1, top panel). A reservoir $2\text{km} \times 1\text{km} \times 300\text{m}$ is located at a depth of 600 m below sea level. The resistivity of the reservoir is 50 Ohm-m. The towed streamer EM survey consists of one survey line, running in the x direction at $y=0$. A horizontal electric dipole transmitter oriented in the x direction with a moment of 1 Am is towed from -10 to 10 km in the x direction at a depth of 10 m below sea level. The transmitter is set to inject 1 Hz EM signal into the sea water at every 300 m. Thirty-one receivers with offsets between 1 km and 7 km are towed at a depth of 100 m and measure the in-line electric fields at a frequency of 1 Hz. The data were contaminated with random 10% Gaussian noise.

Totally 67 transmitter positions along the survey line were employed to construct the SA source. The data observed for

the first shot located at -10 km were selected as the reference field. Figure 1, top two panels, shows cross sections of Model 1, and the SA results for a constant DSA in the next left panels, and that for a boxcar DSA in the right panels. The second panels from the top represents the optimal SA data following Yoon and Zhdanov (2015). The third, fourth, and fifth panels from the top show the SA results produced using Huber, bisquare, and L2 norms for the misfit functionals, respectively. The DSA gate is in cyan solid line. The three norms for RSA result in similar SA data, and all are more stable than conventional OSA.

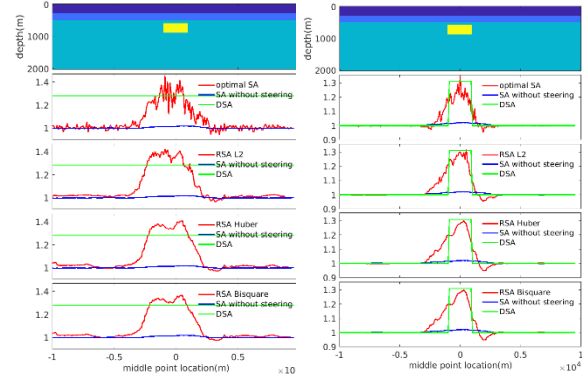


Figure 1: Cross section of model 1 (top panels). The left panels show SA amplitude with a constant DSA, while the right ones are results of a boxcar DSA.

B. Spatial resolution

In the next synthetic study, we considered Model 2 containing two anomalous bodies with different spatial distances to demonstrate the spatial resolution power of the RSA method. Model 2 consists of a 300 m seawater layer with a resistivity of 0.33 Ohm-m, the second layer of 200 m thickness with resistivity of 1 Ohm-m, the third 3 Ohm-m layer with the depth from 500 to 800 m, and a base of 8 Ohm-m. Two reservoirs of the same size, $2\text{km} \times 1\text{km} \times 0.3\text{km}$ with the resistivity of 50 Ohm-m are buried at a depth from 900 to 1200 m. They are aligned with each other in the y direction centered at $y=0$. In our model study, we gradually decrease the separation between the two reservoirs from 2.5 km to 1 km. The observed data were all processed using different versions of the SA method.

We use the same survey design as for Model 1. Figure 2 shows the SA results for four different spatial distances, 2.5 km, 2 km, 1.5 km, and 1 km, respectively. The solid black lines denote RSA results with robust Huber norm. The solid green lines are the RSA results with L2 norm. The conventional OSA results (Zhdanov et al., 2017) are represented by the solid red lines. The SA without steering are shown by the solid blue lines. The results demonstrate that the RSA method generally has better spatial resolution than OSA method. At the same time, for the RSA method

Robust optimal synthetic aperture imaging of towed streamer electromagnetic data

with different norms, the robust norms work a little bit better than the L2 norm.

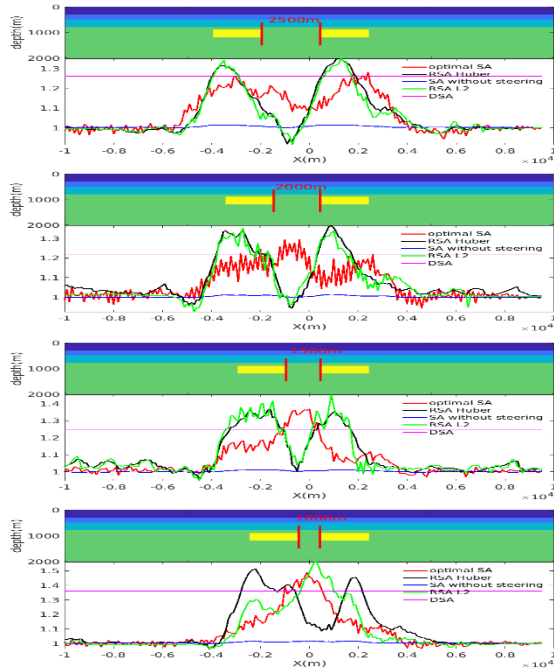


Figure 2: SA results for models of decreasing reservoirs' distance

C. Salt dome model

In this synthetic study, a realistic marine Model 3 contains a salt dome and a fault structure. There is a resistive layer embedded in the conductive basement. The layer is mostly flat but folded to a deeper depth in the northwest. The highly resistive salt dome is located in the eastern part of the survey area. The resistive layer is uplifted around the salt dome. Figure 3 presents a 3D view of the model.

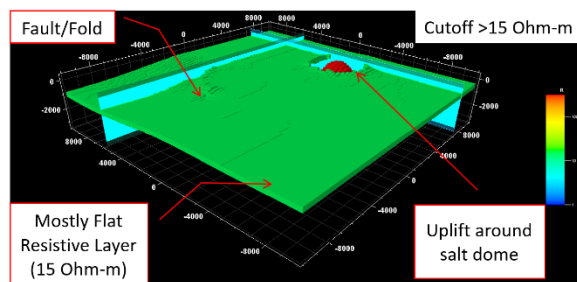


Figure 3: 3D view of Model 3 with a cutoff value of 15 Ohm-m.

A 3D survey consists of 18 survey lines with spacing of 1000 m designed to image the geology. The transmitter is oriented in the x direction and towed from $x=-9000$ m to

$x=9000$ m with a shot interval of 250 m. The EM signal of 7 frequencies from 0.2003 Hz to 3.0049 Hz is transmitted and received. The in-line electric field was synthesized with the integral equation method and contaminated with 10% of Gaussian noise.

We chose the data corresponding to the most southeast shot as the reference field and applied the four different SA methods (OSA and RSA with three different norms) to the synthetic data. As a result, we obtained the SA data for all the survey lines and frequencies. Figures 4 presents, as an example, the amplitudes of the synthetic aperture data at the frequency of 3.0049 Hz. The feature of the salt dome and the fault are well characterized and clearly enhanced in this figure. T

his is very important for offshore HC exploration, in which scenario, the targets are usually buried deep in the sea bottom.

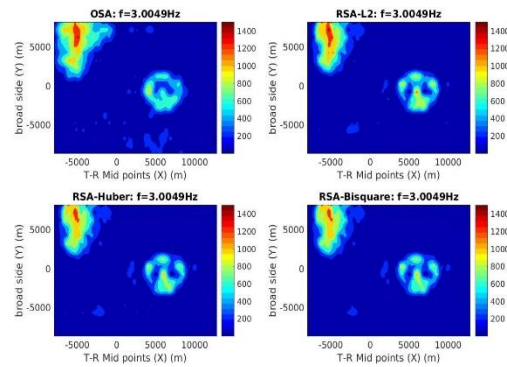


Figure 4: Maps of amplitude of SA data. Left top panel: OSA method. Left bottom and right panels: RSA method with Huber

Conclusions

We have developed a robust synthetic aperture method by applying a robust smoothing to the background field and robust interpolation of the fields from the real local receiver positions to virtual ones. We have also developed and applied a robust inversion scheme to determine the RSA weights using the robust norms. The results of synthetic model study have demonstrated that, RSA method not only is more stable to noise in the data, but also has a better spatial resolution with respect to the sea-bottom geoelectrical structures.

Acknowledgements

The authors acknowledge support from the University of Utah's Consortium for Electromagnetic Modeling and Inversion (CEMI) and TechnoImaging.

Robust optimal synthetic aperture imaging of towed streamer electromagnetic data

References

- Fan, Y., R. Snieder, E. Slob, J. Hunziker, J. Singer, J. Sheiman, and M. Rosenquist, 2010, Synthetic aperture controlled source electromagnetics: *Geophysical Research Letters*, 37, (13), L13305, doi: 10.1029/2010GL043981.
- Fan, Y., R. Snieder, E. Slob, J. Hunziker, J. Singer, J. Sheiman, and M. Rosenquist, 2012, Increasing the sensitivity of controlled-source electromagnetics with synthetic aperture: *Geophysics*, 77, (2), E135-E145, doi: 10.1190/geo2011-0102.1.
- Knaak, A., R. Snieder, Y. Fan, and D. Ramirez-Mejia, 2013, 3D synthetic aperture and steering for controlled-source electromagnetics: *The Leading Edge*, 32, (8), 972-978, doi: 10.1190/tle32080972.1.
- Mattsson, J., and F. Engelmark, 2013, Optimized synthetic aperture sensitivity enhancement of a deep EM marine target: 75th Conference and Exhibition, EAGE, Extended Abstracts.
- Stuart, C., 2011, Robust regression: Report, Durham University.
- Tarantola, A., 2005, Inverse problem theory and methods for model parameter estimation: Society for Industrial and Applied Mathematics.
- Yoon, D., and M. S. Zhdanov, 2015, Optimal synthetic aperture method for marine controlled-source EM surveys: *IEEE Geoscience and Remote Sensing Letters*, 12, (2), 414-418, doi: 10.1109/LGRS.2014.2345416.
- Zhdanov, M. S., D. Yoon, and J. Mattsson, 2017, Rapid imaging of towed streamer EM data using the optimal synthetic aperture method: *IEEE Geoscience and Remote Sensing Letters*, 14, (2), 262-266, doi: 10.1109/LGRS.2016.2637919.
- Zhdanov, M. S., 2015, Inverse theory and applications in geophysics (Second Edition): Elsevier.
- Zhdanov, M. S., 2018, Foundations of geophysical electromagnetic theory and methods (Second Edition): Elsevier.

REFERENCES

- Fan, Y., R. Snieder, E. Slob, J. Hunziker, J. Singer, J. Sheiman, and M. Rosenquist, 2010, Synthetic aperture controlled source electromagnetic: *Geophysical Research Letters*, **37**, L13305, <https://doi.org/10.1029/2010GL043981>.
- Fan, Y., R. Snieder, E. Slob, J. Hunziker, J. Singer, J. Sheiman, and M. Rosenquist, 2012, Increasing the sensitivity of controlled-source electromagnetics with synthetic aperture: *Geophysics*, **77**, no. 2, E135–E145, <https://doi.org/10.1190/geo2011-0102.1>.
- Knaak, A., R. Snieder, Y. Fan, and D. Ramirez-Mejia, 2013, 3D synthetic aperture and steering for controlled-source electromagnetic: *The Leading Edge*, **32**, 972–978, <https://doi.org/10.1190/tle32080972.1>.
- Mattsson, J., and F. Engelmark, 2013, Optimized synthetic aperture sensitivity enhancement of a deep EM marine target: 75th Annual International Conference and Exhibition, EAGE, Extended Abstracts, <https://doi.org/10.3997/2214-4609.20130964>.
- Stuart, C., 2011, Robust regression: Report: Durham University.
- Tarantola, A., 2005, Inverse problem theory and methods for model parameter estimation: Society for Industrial and Applied Mathematics.
- Yoon, D., and M. S. Zhdanov, 2015, Optimal synthetic aperture method for marine controlled-source EM surveys: *IEEE Geoscience and Remote Sensing Letters*, **12**, 414–418, <https://doi.org/10.1109/LGRS.2014.2345416>.
- Zhdanov, M. S., 2015, Inverse theory and applications in geophysics, 2nd ed.: Elsevier.
- Zhdanov, M. S., 2018, Foundations of geophysical electromagnetic theory and methods, 2nd ed.: Elsevier.
- Zhdanov, M. S., D. Yoon, and J. Mattsson, 2017, Rapid imaging of towed streamer EM data using the optimal synthetic aperture method: *IEEE Geoscience and Remote Sensing Letters*, **14**, 262–266, <https://doi.org/10.1109/LGRS.2016.2637919>.